The Spark Plasma Sintering Method Using Laminated Titanium Powder Sheet for Fabricating Porous Biocompatible Implants

Katsuhiro Maekawa[1], Terutake Hayashi[2], Kenichi Hanyu[3], Kazunori Umeda[4], Takashi Murakami[4]

[1]*The Research Center for Superplasticity, Faculty of Engineering, Ibaraki University, Hitachi 316-8511, Japan*
[2]*Micro-mechanical Science Division, Graduate School of Engineering, Osaka University, Suita 565-0871, Japan*
[3]*Graduate School of Science and Engineering, Ibaraki University, Hitachi 316-8511, Japan*
[4]*Advanced Manufacturing Research Institute, AIST, Tsukuba 305-8564, Japan*

(Received March 26, 2006; final form April 19, 2006)

ABSTRACT

Recently, treatment using a titanium implant has become a powerful tool for masticatory dysfunction, in which biocompatibility of titanium is improved by porous coating and alkali treatment. The present study aims to develop a dental implant with interconnected pores which enable tissue regeneration. The implant can be fabricated by a combined technology of rapid prototyping with spark plasma sintering (SPS) using titanium sheet made of a pure powder. The present study reports the evaluation of basic properties of the laminated titanium sheet that has been sintered by the SPS method, followed by the investigation of a technology for controlling internal cell structures. In particular, the use of NaCl powder is essential for retaining the shape of pores.

Keywords: spark plasma sintering, porous metals, titanium, implant, rapid prototyping

1. INTRODUCTION

Porous metals and alloys have various applications such as lightweight structures and filters, since they possess sophisticated properties, including a large surface area, low density and a high thermal insulation, in comparison to conventional materials. Porous titanium especially draws attention as a structural material for bone substitutes and dental implants, because of intrinsic natures of lightweight and biocompatibility.

Precise control over scaffold material, porosity and internal pore architecture are essential for tissue engineering. By adding osteogenic growth factors to synthetic bone substitutes, new bone fabrication could be increased and the clinical outcome improved /1/. After undergoing specific chemical and thermal treatments, porous bioactive titanium induces bone formation without the need of additional osteogenic cells or osteoinductive agents /2/.

Recently, moldless manufacturing techniques, known as rapid prototyping (RP) or layered manufacturing /3/, have been successfully used to fabricate complex scaffolds /4/. Titanium cranioplasty plates are manufactured using the methods of three-dimensional computer modeling from CT scan data, computer-driven milling and selective laser sintering /5/. By coupling RP with conventional sponge scaffold fabrication procedures, methods for casting polymer-ceramic scaffolds that contain designed and controlled locally porous and globally porous internal architectures have been developed /6/. The issue is how to control a

porous structure so as to be best for bone ingrowth and osteoconductivity /7, 8/.

The purpose of the present study is to establish a process of fabricating porous biocompatible implants by employing the spark plasma sintering (SPS) method. The novelty lies in the use of a thin sheet made of a pure titanium powder with organic binders and its lamination to form three-dimensional (3D) sophisticated internal as well as external structures without conventional machining. The present paper reports basic properties of the laminated titanium sheet sintered by SPS, followed by the investigation of a technique for the fabrication of a 3-D internal structure.

2. POROUS IMPLANT DESIGN AND FABRICATION

Rapid prototyping technology has given the product designer access to a vast arsenal of tools and technologies unprecedented in the history of manufacturing. The incredible pace of desktop computing with the market availability of 3D software and the development of rapid prototyping technology allows product design to engage more freely with new ideas, to produce prototypes and to carry out thorough testing in a shorter time. As a step beyond rapid prototyping using a low-strength material like plastics, RP-based direct fabrication using metals and ceramics has lately attracted considerable attention /9, 10/.

The principle of RP is schematically shown in Fig. 1. A 3D-CAD model is converted into an STL format that approximates the surfaces of the model by polygons. The STL model is sliced into layers of cross-sections, and each cross-section is systematically substantiated through the solidification of either liquid or powder and then joined to form a 3D model.

On the other hand, the recent widespread use of the spark plasma sintering method is attributed to such benefits as the generation of spark plasma, rapid rates of Joule heating, and intrinsic field effects on mass transport. High energy due to spark plasma enables sintering at a lower temperature region and a short time of 5-20 minutes. These characteristics can develop the fabrication of porous structures for implants, as shown in Fig. 2.

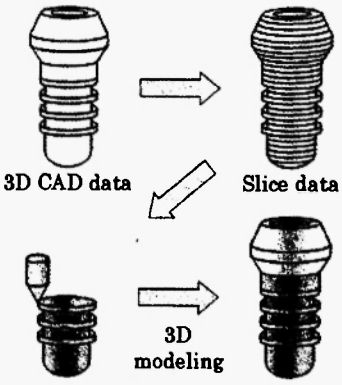

Fig. 1: Fabrication of implant shape by rapid prototyping.

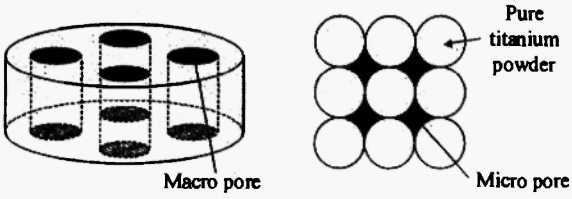

Fig. 2: Fabrication of pore structure by spark plasma sintering.

The method proposed in this research is a combined technology of SPS with rapid prototyping or layered manufacturing. Figure 3 shows a schematic diagram of the 3D modeling process. A sheet of titanium powder is formed as thick as about 200 μm by the mask printing method /11/. The sheet is processed to form a two-dimensional shape by laser cutting, and then laminated to build a three-dimensional object. Finally, a stack of the titanium layers is packed into a carbon mold and sintered by the SPS process.

3. BASIC CHARACTERISTICS OF SPS PARTS

3.1 Experimental method

A pure titanium powder of an average diameter of 83μm was used to form sheet by means of the processes depicted in Fig. 3 (a)-(c). The titanium sheet has a thickness of 206±22 μm and a porosity of 56±5 %. A pulsed Nd:YAG laser beam was irradiated to cut the sheet under an average power of 1.68 W and a scan speed of 3.33 mm/s. Ten pieces of sheet having an

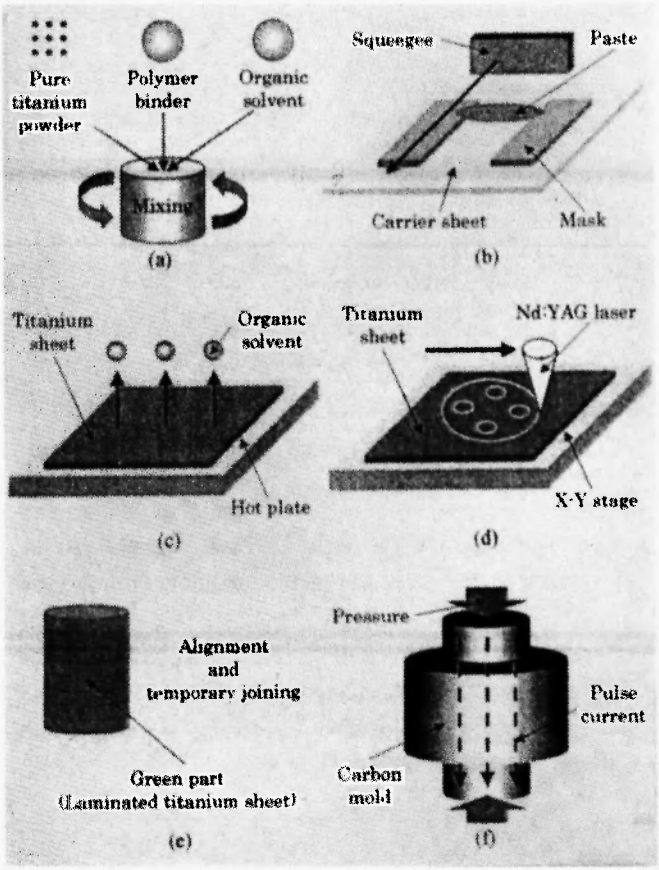

Fig. 3: Schematic diagram of three-dimensional modeling process proposed.

outside diameter of 14.5 mm were stacked to form a columnar specimen. This green part was filled into a carbon mold, and then sintered with SPS equipment under a pressure of 17 MPa and a holding time of 5 min. The sintering temperature was varied from 400 to 800 °C to investigate the behavior of sintering.

Table 1 lists the experimental conditions used: pressure with no sintering (A), normal sintering (B) and sintering with space-holding particles (C). An NaCl powder smaller than 90 μm was used as a spacer.

Dimensional accuracy of the SPS part was evaluated by measuring a rate of in-plane (X-Y plane) expansion, a rate of longitudinal (Z direction) shrinkage, and porosity. Variation of sintered structures was examined with an SEM.

Table 1
Experimantal conditions.

Condition A	Pressure with no sintering
Condition B	Normal sintering
Condition C	Using space-holding particles

3.2 Results and discussion

At the stage of laser cutting, the green sheet has only a -20 μm discrepancy from a set value. Such a precise control is due to a low laser power used to melt the organic binder and dissolve bonding between titanium powders. No thermal distortion took place.

In the course of the SPS process, the specimen was shrunk as much as 46-52 % in the Z direction. It is found that most of the shrinkage is due to the pressure applied before energized. Shrinkage by sintering ranged from 6 to 11 %. A rate of expansion in the X-Y plane depends on the diameter of a mold. In this case, every specimen expanded to 15 mm in diameter regardless of sintering temperature. The rate of expansion is 4.7-5.0 %, or from 14.31±0.02 to 15 mm in diameter. Porosity of the sintered part is 14 % at 650 °C and 8 % at 700 °C.

Figure 4 compares surface morphology with varying sintering temperatures: (a) 650 °C and (b) 700 °C. The SEM micrographs reveal that the shape of titanium powder is maintained without grain growth, and small pores exist at 650 °C. On the contrary, a full sintering proceeds at 700 °C. In order to keep micro pores in the specimen, the sintering temperature should be come under control of below 650 °C.

Figure 5 shows the titanium sheet used in the experiment and the results obtained under the conditions listed in Table 1. The macro pores or circular spaces

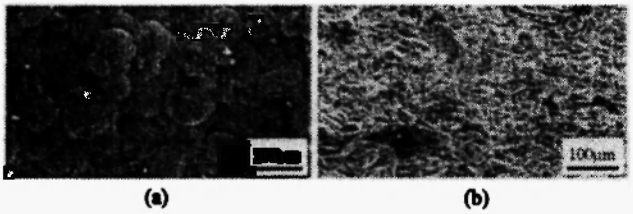

Fig. 4: Cross-sectional SEM micrograph of sintered titanium sheet at sintering temperatures of (a) 650 °C and (b) 700 °C.

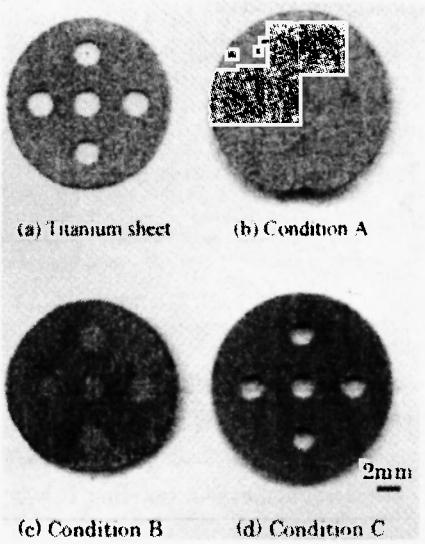

Fig. 5: Titanium sheet and SPS parts at various conditions.

disappear due to pressuring before sintering, as shown in Fig. 5 (b) and (c), whereas they are retained as they are by using the NaCl spacer, as shown in Fig. 5 (d).

Figure 6 compares the variation of distance between pores when sintered under the condition C. The symbols A-D indicate the places where the distance was measured. Every distance is increased according to pressurization, whereas the pore diameter is decreased from 2.0 mm to 1.4 mm, or the rate of shrinkage is 37%.

Furthermore, dimensional accuracy of the macro pores was evaluated by using a stack of 10-piece titanium-sheet with varying pore size of 0.5-4.0 mm. Figure 7 shows the sintered parts with changing pore

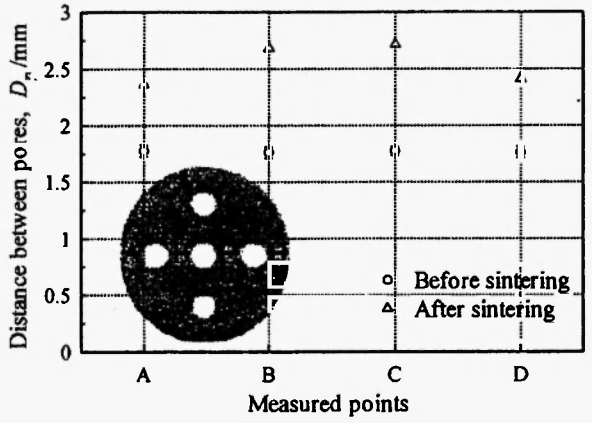

Fig. 6: Variation of distance between pores.

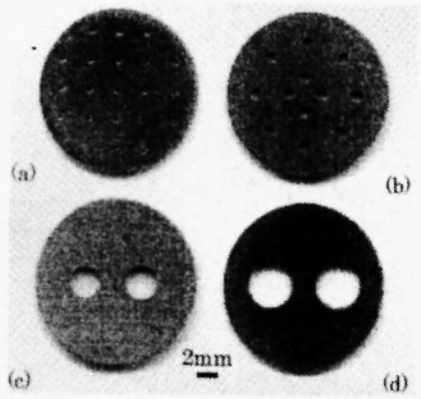

Fig. 7: SPS parts with changing macro pore diameter: (a) 0.5, (b) 1.0, (c) 3.0, (d) 4.0 mm.

size. The macro pores with 0.5 mm diameter can be produced by the proposed method together with the use of NaCl as a spacer. Figure 8 indicates the variation of distance between pores. The rate of expansion ranges from 15 to 30 % with changing pore size. The variation of pore size is adjustable by taking shrinkage into account, as shown in Fig. 9.

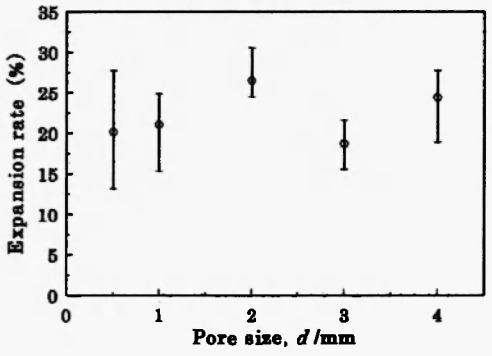

Fig. 8: Variation of distance between pores when initial pore diameter is changed.

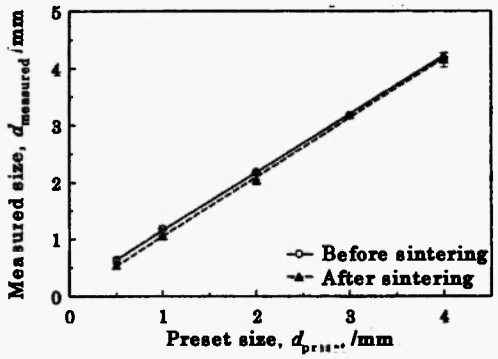

Fig. 9: Relation between measured pore size and preset one.

4. FABRICATION OF OPEN-CELL AND CLOSED-CELL STRUCTURES

4.1 Experimental method

Two kinds of titanium circular sheet having macro pores of 3.0 and 7.0 mm in the center were prepared by the mask printing method and laser cutting. Each 20 pieces of sheet was piled up concentrically in an alternative fashion to form 100 pieces of an open-cell green part. On the other hand, a closed-cell green part was formed such a manner that 20 pieces of 3.0 mm-pore sheet were replaced by the same pieces of sheet without macro pores. Again, these macro pores were filled with NaCl powder and pressed in a carbon mold at around 11 MPa until SPS was employed under a sintering temperature of 650 °C and a holding time of 5 min.

An ultrasonic cleaner was used to dissolve NaCl powder from the sintered specimen in pure water for 30 min. Then, the specimen was cut in half in a longitudinal direction. Dimensional accuracy of the sintered cells was measured with an optical microscope.

4.2 Results and discussion

Table 2 summarizes the basic properties of the sintered cell structures: the rate of shrinkage in the Z direction, the rate of expansion in the X-Y plane, and the porosity calculated by the measured volume and weight. These values are almost the same in both open-cell and closed-cell structures. Figure 10 shows the cross-sectional view of the cut specimens. Internal pore structures are maintained with a reasonable accuracy.

Table 2
Basic properties of sintered cell structures.

	Open-cell	Closed-cell
Rate of shrinkage in thickness	44.0 %	45.2 %
Rate of in-plane expansion	6.6 %	6.5 %
Porosity	27 %	26 %

Figures 11 and 12 show the variations of macro-pore diameter and thickness in an axial direction,

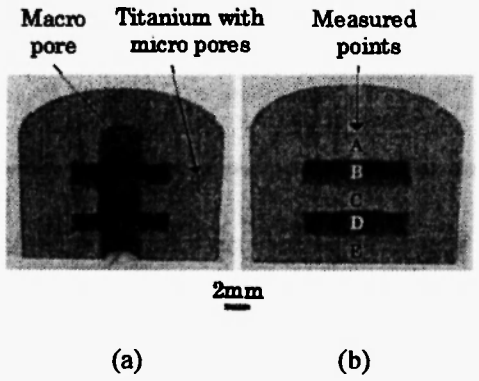

Fig. 10: Cross-sectional view of (a) open-sell and (b) closed-cell structures.

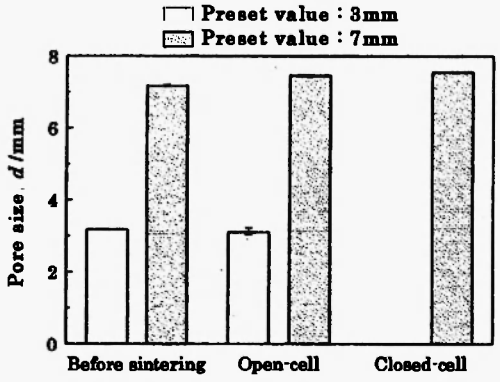

Fig. 11: Variation of pore size before/after sintering.

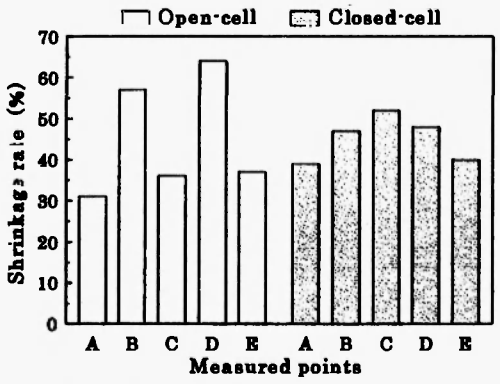

Fig. 12: Variation of thickness at measured points in Fig. 10.

respectively. The diameter shows a small discrepancy before and after sintering: a shrinkage of 80 μm as for the 3.0 mm pore. In the case of the 7.0 mm pore, there appear an expansion of 290 μm for the open cell and a slightly higher expansion of 380 μm for the closed cell.

As can be seen in Fig. 12, the highest rate of shrinkage is 64 % at the measured point D as for the open cell, whereas that of the closed cell is 52 % at the center C. It seems that this difference arises from the filling method of NaCl powder; the salt was filled into the open-cell green part after laminating the whole body. In order to improve dimensional accuracy of macro pores, the volume of salt as well as the filling method should be normalized. In terms of thickness in a radial direction, it increases by 420±20 μm at the pore site of 3.0 mm, while it also expands by 210±30 μm at the pore site of 7.0 mm in both open-cell and closed-cell structures.

Although the cross-sections shown in Fig. 10 become smooth in the course of cutting in half, a number of micro pores smaller than 20 μm, such as those that can be observed in Fig. 4 (a), are included within the whole sintered body. When the closed-cell part was cut in half, the NaCl powder had gone by the preceding ultrasonic cleaning. This fact explains the existence of micro pores in the SPS sintered parts.

Further study includes more precise control of internal cell structures, and the investigation of mechanical properties and biocompatibility of the implant fabricated by the proposed method.

5. CONCLUSIONS

(1) For the purpose of fabricating porous biocompatible implants, a combined technology of spark plasma sintering with rapid prototyping or layered manufacturing has been proposed. The novelty lies in the laser cutting of pre-formed titanium powder-sheet and the use of NaCl powder as a spacer during sintering.

(2) Micro pores of around 20 μm can be produced under a sintering temperature of below 650 °C and a holding time of 5 min.

(3) Interconnected pores or macro pores of around 2 mm in diameter are successfully fabricated using the NaCl spacer.

(4) Both open-cell and closed-cell structures can be designed and assembled with the proposed method with a reasonable accuracy.

REFERENCES

1. S. A. Clarke, R. A. Brooks, P. T. H. Lee and N. Rushton: *J. of Orthopaedic Res.*, **22**, 1016-1024 (2004).
2. S. Fujibayashi, M. Neo, H. M. Kim, T. Kokubo and T. Nakamura: *Biomaterials*, **25**, 443-450 (2004).
3. D. L. Bourell, H. L. Marcus, J. W. Barlow and J. J. Beaman: *Int. Jour. of Powder Metallurgy*, **28**, 369-381 (1992).
4. W. H. Dietmar, S. Michael and V. R. Makarand: *Trends in Biotechnology*, **22**, 354-362 (2004).
5. M. A. Stoodley, J. R. Abbott and A. Simpson: *J. of Clinical Neuroscience*, **3**, 149-155 (1996).
6. J. M. Taboas, R. D. Maddox, P. H. Krebsbach and S. J. Hollister: *Biomaterials* **24**, 181-194 (2003).
7. J. M. Williams, A. Adewunmi, R. M. Schek, C. L. Flanagan, P. H. Krebsbach, S. E. Feinberg, S. J. Hollister and S. Das: *Biomaterials*, **26**, 4817-4827 (2005).
8. F. Watari, A. Yokoyama, M. Omori, T. Hirai, H. Kondo, M. Uo and T. Kawasaki: *Composites Science and Technology*, **64**, 893-908 (2004).
9. L. Lü, J. Fuh, and Y. -S. Wong: *Laser-Induced Materials and Processes for Rapid Prototyping*, Kluwer Academic Publishers (2001).
10. K. Maekawa: Proc. *2nd Int. Conf. on Rapid Prototyping and Manufacturing*, Beijing, August 19-20, 304-313 (2002).
11. K. Hanyu, M. Tamura, T. Hayashi and K. Maekawa: *Proc. JSME Annual Meeting*, 483-484 (2004).